

Correlated piecewise diffusion of a Ge ad-dimer on the Si(001) surface

Zhong-Yi Lu, Cai-Zhuang Wang, and Kai-Ming Ho

Ames Laboratory-U.S. DOE and Department of Physics and Astronomy, Iowa State University, Ames, Iowa 50011

(Received 4 May 2000)

We have performed extensive first-principles calculations to study the binding and diffusion of a Ge ad-dimer on the Si(001) surface. The diffusion of a Ge ad-dimer along the lowest-energy-barrier pathway is found to be piecewise but with strong correlation, and its energy barrier is 0.77 eV. Such a correlated piecewise diffusion pathway is also found to be favored by a Si ad-dimer on Si(001), with an energy barrier of 1.02 eV in excellent agreement with experimental measurements.

Homoepitaxial growth of Si on the Si(001) surface has been intensively studied in the past decade¹⁻³ due to the technological importance of Si(001) surface in microelectronic industry. Recently, heteroepitaxial growth of Ge on Si(001) has also attracted considerable interest because Ge/Si heterostructures are expected to have exciting potential applications in new electronic devices in the near future.⁴ In order to understand the mechanism and have a better control of heteroepitaxial (homoepitaxial) growth of Ge (Si) on Si(001), knowledge about the binding and diffusion of Ge (Si) ad-dimers on Si(001) at atomistic levels is very useful and desirable.

Both experimental^{2,3} and theoretical⁵⁻⁷ studies indicate that the diffusion of a Si ad-dimer on Si(001) is strongly anisotropic: the ad-dimer prefers to diffuse along the top of dimer row. By contrast, the diffusion of a Ge ad-dimer on Si(001) has not been studied.

Recently we have carried out extensive first-principles calculations to study a Ge ad-dimer on Si(001). In this paper we report the results of our calculations on the binding energies and structures of a Ge ad-dimer on Si(001) and the diffusion mechanism of the ad-dimer along the top of the dimer row. Our results indicate that the diffusion of a Ge ad-dimer on the top of the dimer row on Si(001) is piecewise. However, this piecewise diffusion of the two Ge atoms is not random but strongly correlated.

Our calculations were performed using an *ab initio* pseudopotential plane-wave self-consistent method in the framework of the density-functional theory within the local-density approximation (LDA).⁸ The Kohn-Sham orbitals were expanded in plane waves with an energy cutoff of 12 Ry. We modeled the surface by a periodically repeated slab along three directions. The slab contains eight Si layers with 16 Si atoms per layer, and a vacuum region of at least 12.5 Å thickness in the direction normal to the surface. The top surface layer is arranged in a 4×4 unit cell with $c(2 \times 4)$ reconstruction while the bottom surface layer is passivated by 32 H atoms. A Ge (Si) dimer was put on the top of the surface when studying Ge (Si) ad-dimer binding and diffusion. Thus there are a total of 128 Si atoms, 2 Ge (Si) adatoms, and 32 H atoms in the slab. The Si atoms in the bottom surface layer and the H atoms are frozen while all other atoms are allowed to relax until the forces are less than 0.01 eV/Å. A set of four special *k* points is chosen to sample the square surface Brillouin zone.⁹

Previous calculations⁵⁻⁷ suggest there are four principal binding configurations for a Si ad-dimer on Si(001), as shown in Fig. 1. Dimers *A* and *B* sitting on the top of a dimer row are reported to be energetically favorable and very close in energy. Experimental measurements¹⁰ show that dimer *A* is energetically about 0.059 eV lower than dimer *B*. However, in LDA calculations, the energy ordering of dimers *A* and *B* is sensitive to the choice of exchange-correlation (XC) functional. Specifically, the calculations using Ceperley-Alder (CA) XC functional¹¹ favor dimer *B* while the calculations using Wigner interpolation formula¹² for the XC functional obtain results in agreement with experiments.^{5,6}

Since there are no reliable experimental data regarding the energetics and geometries of Ge ad-dimers on Si(001), and since the CA functional is most commonly used in LDA calculations, we primarily adopted the CA XC functional with the parametrization of Perdew and Zunger¹¹ while the

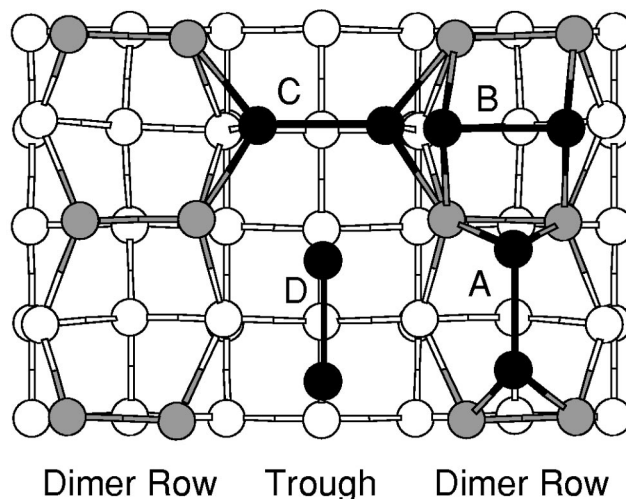


FIG. 1. Schematic drawing of the four principal binding configurations for a Si or Ge ad-dimer on Si(001). The black filled circles represent the ad-dimers, the gray filled circles represent the dimer atoms in the top surface layer, and the open circles represent the atoms below the surface layer. Here the two ad-dimers sitting on the top of a dimer row are called dimer *A* (parallel to the dimer row) and *B* (perpendicular to the dimer row), the others in the trough between two dimer rows are called dimer *C* (perpendicular to the dimer row) and *D* (parallel to the dimer row), respectively. The energies for these ad-dimers are reported in Table I.

TABLE I. Calculated energies E (eV/dimer), buckling lengths b (Å), bond lengths d (Å), and buckling angles ω (degree) for Si and Ge ad-dimers A , B , C , and D on Si(001), schematically shown in Fig. 1. Here the numbers in parentheses correspond to the calculations using the Wigner formula. And the energy of dimer A sets to zero.

	E	b	d	ω
Si				
A	0 (0)	0.47 (0.46)	2.346 (2.367)	11.7° (11.2°)
B	-0.023 (0.053)	0.00 (0.00)	2.310 (2.323)	0.0° (0.0°)
C	0.107 (0.215)	0.01 (0.01)	2.474 (2.503)	0.3° (0.2°)
D	0.890 (0.955)	0.31 (0.30)	2.297 (2.312)	7.7° (7.5°)
Ge				
A	0 (0)	0.49 (0.45)	2.542 (2.537)	11.1° (10.2°)
B	0.017 (0.082)	0.00 (0.00)	2.468 (2.461)	0.0° (0.0°)
C	0.159 (0.225)	0.03 (0.04)	2.670 (2.672)	0.7° (0.9°)
D	0.878 (0.938)	0.55 (0.48)	2.456 (2.474)	12.9° (11.3°)

electron-ion interaction is described by norm-conserving pseudopotentials¹³ in the Kleinman-Bylander form¹⁴ with s and p nonlocality. We then also checked the calculation results using the Wigner formula for the XC functional instead of the CA functional. In the latter case, for consistency we generated new Ge and Si pseudopotentials using the Troullier-Martins approach¹⁵ with the Wigner formula for the XC functional.

We first undertook calculations for Si ad-dimers A , B , C , and D on Si(001), similar to those in Refs. 5 and 6 but with a larger slab, higher kinetic energy cutoff, and more k points in the surface Brillouin-zone sum. Our results, reported in Table I, are basically similar to the previous LDA calculations in Refs. 5 and 6, but have a better agreement with experiments when the Wigner formula is used.

We then carried out calculations for a Ge ad-dimer on Si(001), and found that a Ge ad-dimer also has four principal binding configurations located in A , B , C , and D positions shown in Fig. 1. The calculated results are also summarized in Table I. As we can see from Table I, both Ge ad-dimers and Si ad-dimers are quite similar in energy ordering and structure geometry, especially in the Wigner formula case. For a Ge ad-dimer, configuration A is favored by both the CA functional and the Wigner formula, followed by configurations B , C , and D . The relative energies of dimers B , C , and D with respect to dimer A obtained by using the CA functional are smaller than those by using the Wigner formula (on average by about 0.064 eV for Ge ad-dimers, and about 0.083 eV for Si ad-dimers). Such a systematic energy shift can cause the energy ordering reverse for Si ad-dimers A and B , but not enough for the Ge ad-dimers. It is also interesting to note that dimers B and C are essentially unbuckled while dimers A and D are largely buckled. Our calculation results show that the unbuckled Si and Ge dimers A are energetically 0.140 and 0.043 eV higher than the buckled ones, respectively.

Diffusion of dimer B on the top of dimer row is obviously much more costly in energy than the diffusion of dimer A because the former will break more bonds and induce larger stress. We thus focus here on the diffusion of dimer A . In order to search for the diffusion pathway of dimer A on the

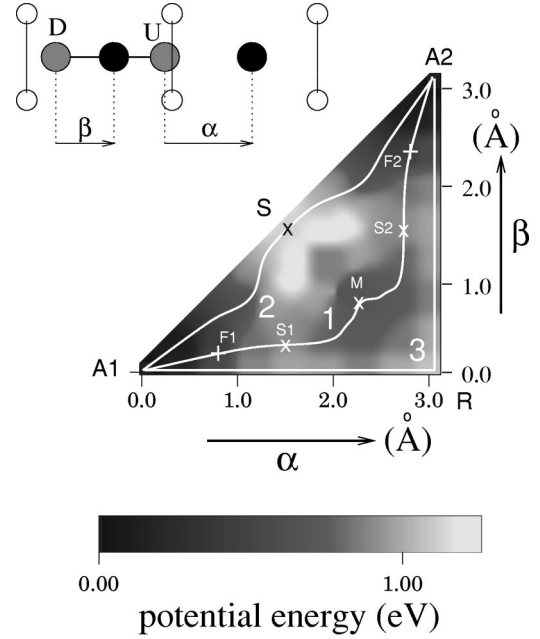


FIG. 2. Potential energy surface for the diffusion of a Ge ad-dimer on the top of dimer row on Si(001). Here U and D indicate the up and down atoms of dimer A in the initial configuration $A1$ respectively. Correspondingly, α and β denote the displacements of the U and D atoms along the dimer row from their initial positions, respectively, as schematically illustrated in the upper left inset in which the open circles represent the atoms of the dimer row of Si(001); the two gray filled circles represent the ad-dimer in its initial position $A1$; and the two black filled circles represent the two dimer atoms in an intermediate state. The displacements are in Å, and the energies are in eV. Line 1 represents the lowest-energy-barrier “correlated piecewise” diffusion pathway along which $S1$ and $S2$ are two saddle points, M is a local minimum, $F1$ and $F2$ are two intermediate states, $A1$ and $A2$ are the initial and final states, respectively (both are optimized configurations). All corresponding atomic geometries of $A1$, $F1$, $S1$, M , $S2$, $F2$, and $A2$ are shown in Fig. 3. Line 2 represents the “bonded dimer” diffusion pathway where S indicates one saddle point. The specific energy variations along line 1 and line 2 are shown in Fig. 4. Line 3 represents the “one moving one frozen” diffusion pathway.

top of dimer row on Si(001) as completely as possible, we have performed extensive calculations to map out a potential energy surface (PES). This PES is shown in Fig. 2 as a function of the displacements α and β of the two atoms of the Ge ad-dimer. For convenience, we call the up atom and the down atom of dimer A in the initial configuration $A1$ as U atom and D atom, respectively. α and β denote the displacements of the U atom and the D atom along the dimer row from their initial positions $A1$, respectively, as shown in Fig. 2. In the calculations, the coordinates of the U and D atoms along the dimer row are fixed while all other coordinates are fully relaxed. The PES was generated by a 12×12 grid mesh. Due to the symmetry, actually, there are about 50 independent configurations needed to be computed. Additional configurations were computed around the saddle points in order to get more accurate values for the diffusion barriers. There are three saddle points labeled S , $S1$, and $S2$ and one local minimum labeled M found in the PES. These positions are marked x in Fig. 2. In order to further confirm

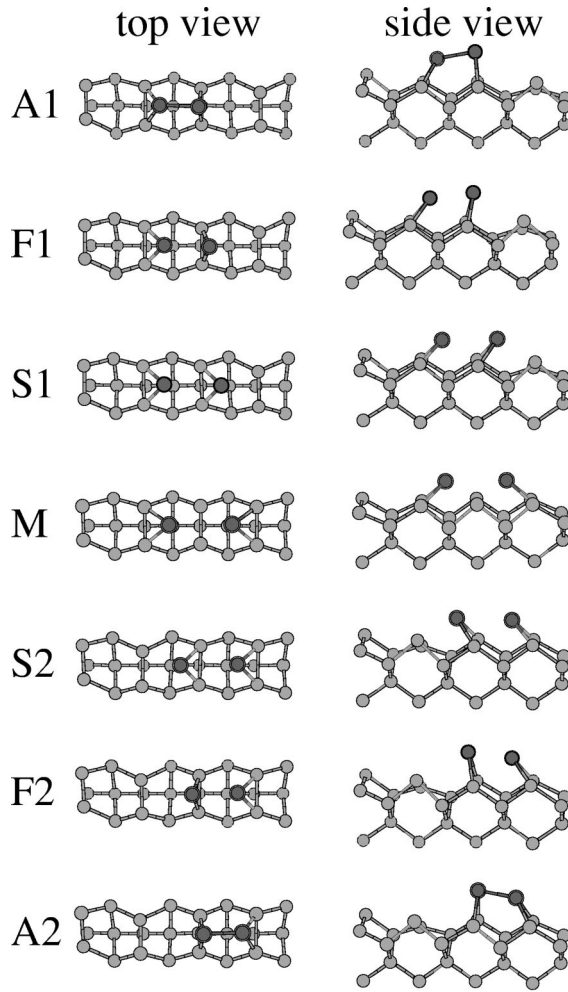


FIG. 3. Principal atomic geometries on the correlated piecewise diffusion pathway represented by line 1 in Fig. 2. The dark filled circles represent two diffusing atoms, the others represent the atoms in or below the top surface layer. Note the bucklings of A1 and A2 are reverse.

these saddle points and local minimum M , we did more calculations by relaxing the configurations from the saddle points. The relaxations resulted in either the local minimum M or the global minimum A1 or A2.

By inspecting the PES in Fig. 2, we find that the most favorable diffusion pathway for a Ge ad-dimer on Si(001) is path 1, which starts from A1, goes through the saddle point S1, the local minimum M and the saddle point S2, to finally reach A2. The corresponding energy variation along path 1 is plotted as the solid line in Fig. 4. Its energy barrier is found to be 0.77 eV, and is located at the two saddle points S1 and S2. The local minimum M has a value of 0.66 eV relative to point A1 (or A2). The corresponding principal atomic configurations along path 1 are displayed in Fig. 3. As we can see from Figs. 3 and 2, the diffusion of the ad-dimer along path 1 exhibits some very interesting features. From A1 to F1, both U and D atoms start to move, but the U atom moves faster than the D atom. From F1 the D atom becomes almost frozen while the U atom crosses the substrate dimer and goes into the neighbor site region, i.e., the system passes through the first saddle point S1 and goes into the local minimum M . From this local minimum M , the situation

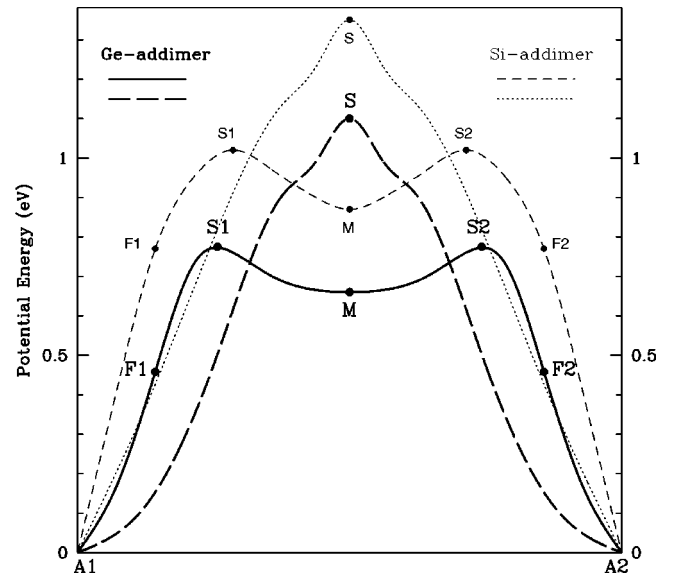


FIG. 4. Specific energy variations of Ge and Si ad-dimers along paths 1 and 2 shown in Fig. 2. The solid line (Ge) and the short dashed line (Si) correspond to path 1 case, and the long dashed line (Ge) and the dot line (Si) correspond to path 2 case. All marked and labeled points correspond to those appearing in Figs. 2 and 3.

swaps between the D atom and the U atom. That is, the U atom becomes almost frozen, while the D atom begins to rapidly move and crosses the substrate dimer to merge with the U atom. The system thus passes through the second saddle point S2 and goes onto F2. Then from F2, the D and U atoms again both move but the D atom moves faster than the U atom until they finally reach A2, a new site of dimer A. Here we would like to point out that in the A2 configuration the U atom becomes a down dimer atom while the D atom becomes an up dimer atom. That is, the dimers in A1 and A2 configurations have reverse buckling with each other, which has been clearly shown in Fig. 3. This diffusion mode is thus clearly piecewise since the dimer bond is broken at a time. As we can see from Fig. 3, at the local minimum M , the U and D atoms have the largest separation along path 1. One may wonder whether the “ U ” and “ D ” atoms will further jump away from each other, starting from M . In order to check this possibility, we carried out calculations by gradually moving one of these two atoms toward the second-next-neighbor site with the other atom being frozen. The energy barrier for this dissociation motion turns out to be 1.27 eV, much larger than the barrier of 0.77 eV along path 1. We therefore see that at the local minimum M , even though the D and U atoms are separated at two neighbor sites without a direct bond, they do have a strong correlation between them. They tend to jump toward each other to form a new dimer A, rather than jump away from each other. It is this reason that we would like to call this diffusion mode “correlated piecewise” rather than simply “piecewise.”

It is worthwhile to discuss other pathways besides path 1. One simple diffusion pathway is path 2 shown in Fig. 2. Its energy variation is shown as the long dashed line in Fig. 4. Along path 2 the U and D atoms are always bonded as a unit. So we may call it “bonded dimer” diffusion. This pathway is essentially similar to the one previously proposed for a Si ad-dimer on Si(001).⁶ This pathway seems very straightforward.

ward but its energy barrier is found to be 1.10 eV, quite larger than that of path 1. Another pathway is the “one moving one frozen” pathway shown as path 3 in Fig. 2 ($A1-R-A2$). Along path 3, from $A1$ to R , the D atom is completely frozen while the U atom first moves into the neighbor site region. Then the U atom becomes completely frozen, and the D atom follows to form a new dimer A in $A2$ position. Its energy barrier was computed to be 1.04 eV at point R shown in Fig. 2.

In order to check the effects of the unit cell size on the results, we repeated calculations for the saddle points $S1$ and S as well as dimer A using a larger 4×8 unit cell (i.e., doubling the 4×4 unit cell along the substrate dimer row). We used the same energy cutoff and equivalent k points as those used in the above calculations. The results show that although the Ge ad-dimer can make the nearest substrate dimers unbuckled, its effects on the next nearest substrate dimers are negligible except at the saddle point $S1$. In that case, the bond length and buckling angle of the next nearest substrate dimer are 2.34 Å and 18° , as compared to 2.32 Å and 19.4° in the absence of the ad-dimer. No notable effects are detected for the farther substrate dimers. The obtained energy barriers are 0.79 and 1.11 eV along paths 1 and 2, respectively, close to the results from the 4×4 unit cell calculations. These results suggest that a unit cell of 4×4 is sufficient for the present study.

Possible piecewise diffusion of a Si ad-dimer on Si(001) has also been suggested.¹⁶ However, the diffusion pathway was not well characterized, particularly, the correlated motion of the two adatoms, similar to the Ge ad-dimer in our calculations, which was also not well examined. In order to further clarify the diffusion of a Si ad-dimer on the top of dimer row on Si(001), we have performed calculations for a Si ad-dimer along the paths similar to those specified in Fig. 2. The calculated energy variations along paths 1 and 2 are plotted in Fig. 4. Our results show that path 1 is still the

favorable diffusion pathway for a Si ad-dimer with an energy barrier of 1.02 eV which is in excellent agreement with experiment.¹⁶ The local minimum M has a value of 0.87 eV, and from M the energy barrier for the dissociation motion was computed to be 1.55 eV, much larger than that for path 1. So path 1 is also strongly correlated for a Si ad-dimer. In comparison, the Si ad-dimer diffusions along paths 2 and 3 have a barrier of 1.35 and 1.28 eV, respectively. The Si ad-dimer diffusion on the top of dimer row was measured by the atom-tracking scanning tunneling microscopy¹⁶ above 360 K. Based on the ratio of diffusion energy barriers between Ge and Si ad-dimers, we expect the Ge ad-dimer diffusion on the top of dimer row could be observable at room or lower temperatures.

Finally, we have also checked the diffusion energy barriers with the Wigner formula instead of the CA functional, and found that both functionals give essentially the same energy barriers.

In conclusion, through the extensive calculations for Ge and Si ad-dimers on Si(001) we find both Ge and Si ad-dimers have similar binding configurations and exhibit similar diffusive behavior along the top of dimer row. Both lowest-energy-barrier diffusion pathways are correlated piecewise, that is, one of the two dimer atoms first jumps into the neighbor site while the other atom is nearly frozen. However, the second atom will then follow to form a new dimer, rather than jump away from each other, due to the correlation between these two atoms. The corresponding energy barriers are 1.02 eV for a Si dimer, and 0.77 eV for a Ge dimer.

Ames Laboratory is operated for the U.S. Department of Energy by Iowa State University under Contract No. W-7405-Eng-82. The calculations in this work were done on National Energy Research Supercomputing Center.

¹For instance, M. Lagally, R. Kariotis, B. Swartzentruber, and Y. W. Mo, *Ultramicroscopy* **31**, 87 (1989); Y. W. Mo, B. Swartzentruber, R. Kariotis, M. Webb, and M. Lagally, *Phys. Rev. Lett.* **63**, 2393 (1989); C. Pearson, M. Krueger, and E. Ganz, *ibid.* **76**, 2306 (1996); J. van Wingerden, A. van Dam, M. J. Haye, P. M. L. O. Scholte, and F. Tuinstra, *Phys. Rev. B* **55**, 9352 (1997).

²Y. W. Mo, J. Kleiner, M. B. Webb, and M. G. Lagally, *Phys. Rev. Lett.* **66**, 1998 (1991).

³D. Dijkkamp, E. J. van Loenen, and H. B. Elswijk, *Proceedings of the 3rd NEC Symposium on Fundamental Approach to New Material Phases*, Springer Series on Material Science (Springer-Verlag, Berlin, 1992).

⁴E. Kaspar, *Curr. Opin. Solid State Mater. Sci.* **2**, 48 (1997).

⁵G. Brocks and P. J. Kelly, *Phys. Rev. Lett.* **76**, 2362 (1996).

⁶T. Yamasaki, T. Uda, and K. Terakura, *Phys. Rev. Lett.* **76**, 2949 (1996).

⁷G. D. Lee, C. Z. Wang, Z. Y. Lu, and K. M. Ho, *Phys. Rev. Lett.*

81, 5872 (1998).

⁸P. Hohenberg and W. Kohn, *Phys. Rev.* **136**, B864 (1964); W. Kohn and L. J. Sham, *ibid.* **140**, A1135 (1965).

⁹S. L. Cunningham, *Phys. Rev. B* **10**, 4988 (1974).

¹⁰B. S. Swartzentruber, A. P. Smith, and H. Jónsson, *Phys. Rev. Lett.* **77**, 2518 (1996); Zhenyu Zhang, Fang Wu, H. J. W. Zandvliet, B. Poelsema, H. Metiu, and M. G. Lagally, *ibid.* **74**, 3644 (1995).

¹¹D. M. Ceperley and B. J. Alder, *Phys. Rev. Lett.* **45**, 566 (1980); J. P. Perdew and A. Zunger, *Phys. Rev. B* **23**, 5048 (1981).

¹²E. Wigner, *Phys. Rev.* **46**, 1002 (1934).

¹³R. Stumpf, X. Gonze, and M. Scheffler, Fritz-Haber-Institut Research Report, 1990 (unpublished).

¹⁴L. Kleinman and D. M. Bylander, *Phys. Rev. Lett.* **48**, 1425 (1982).

¹⁵N. Troullier and J. L. Martins, *Phys. Rev. B* **43**, 1993 (1991).

¹⁶B. Borovsky, M. Krueger, and E. Ganz, *Phys. Rev. B* **59**, 1598 (1999).